MDPI

Article

Experimental Analysis of Nucleation Triggering in a Thermal Energy Storage Based on Xylitol Used in a Portable Solar Box Cooker

Gianluca Coccia [1,*] **, Alessia Aquilanti** [1,2] **, Sebastiano Tomassetti** [1] **, Pio Francesco Muciaccia** [1] **and Giovanni Di Nicola** [1]

1 Department of Industrial Engineering and Mathematical Sciences, Marche Polytechnic University, Via Brecce Bianche 12, 60131 Ancona, Italy; a.aquilanti@pm.univpm.it (A.A.); s.tomassetti@pm.univpm.it (S.T.); p.f.muciaccia@pm.univpm.it (P.F.M.); g.dinicola@univpm.it (G.D.N.)
2 Institute of Construction and Building Materials, Technical University of Darmstadt, Franziska-Braun-Str. 3, 64287 Darmstadt, Germany
* Correspondence: g.coccia@univpm.it; Tel.: +39-071-220-4277

Abstract: Sugar alcohols have interesting thermodynamic properties that make them good options as heat storage materials (HSMs) to be used in solar cookers. Among sugar alcohols, xylitol is affected by severe supercooling that can significantly alter its usefulness in thermal energy storage (TES) systems. To overcome the supercooling issue, in this work the thermal behavior of a xylitol-based TES installed in a portable solar box cooker was investigated experimentally. The solar cooker has a 4.08 concentration ratio and the TES is a double-pot system filled with 2.5 kg of commercial-grade xylitol. The TES includes a manual mixing device that can be used to trigger the nucleation of xylitol. The effectiveness of the TES system with and without triggering was assessed through several outdoor tests, divided into heating and cooling phases, using silicone oil as absorbing media. It was found that the average load cooling time, in the temperature range of the test fluid from 110 to 80 °C, increased by about 346% when the solar cooker was equipped with the xylitol-triggered TES. The mixing device can therefore be considered an effective solution for regarding xylitol as an actual and performing phase change material.

Keywords: sugar alcohol; supercooling; nucleation triggering; heating phase; cooling phase; thermal energy storage; phase change material

1. Introduction

One of the best and most promising ways to exploit solar energy is represented by solar cooking. It is well-known that many developing countries benefit from abundant solar radiation, with an average intensity of illumination that every day lies in the range of 5–7 kW/m^2, and more than 275 days of sunshine in a year [1–3]. Nevertheless, solar radiation is variable by nature and depends on the day–night cycle, seasons and meteorological conditions, thus it is not able to cover alone the usual domestic demand for energy.

One way to compensate for this intermittence would be to store the excess of thermal energy converted from solar energy, in order to use it when solar radiation is absent. In recent years, there has been an ever-growing interest in studying new methods for storing energy, such as thermal, electrical, chemical and mechanical energy storages [4–6]. Thermal energy storages (TESs), in particular, can take advantage of either the sensible or the latent heat associated to the physical phase of specific substances, called heat storage materials (HSMs). As suggested by their name, the latent-heat-based substances, also referred to as phase change materials (PCMs), can continuously change their physical state to absorb or release their latent heat generally over a narrow temperature range. The physical phases involved in the process are usually the solid and the liquid forms. The combination of a relevant amount of latent heat released and the thermal stabilization derived from the

quasi-constant temperature phase transition can significantly enhance the use of solar cooking. In fact, PCM-based TESs integrated in solar cookers allow the absorption of solar energy during the heating process and to release the collected thermal energy during the cooling process, keeping the food temperature steady.

Numerous studies demonstrated that solar cookers with embedded TESs, especially if based on PCMs, constitute a valuable alternative to more traditional cooking solutions that involve the usage of mostly used and environmentally harmful fuels (e.g., firewood, manure and agricultural waste, coal) [7–9]. In this way, a moderate use of firewood would help to preserve the ecosystem while animal manure could be used as natural fertilizer to help agriculture.

Sugar alcohols (SAs), also called polyalcohols or polyols, belong to the family of low molecular weight carbohydrates and their general formula is $C_nH_{2n+2}O_n$. While some SAs are of natural origin and can be found in various fruits and vegetables, many SAs are chemically derived from the reduction of carbohydrates. They are non-flammable, non-toxic, and most of them are cost-effective [10]. Although they are usually considered non-corrosive [10,11], it was shown that some SAs are prone to corrosion [12].

In relation to their melting temperatures and thermophysical properties, some SAs are considered suitable to be used as PCMs in solar cookers for applications in the low–medium temperature range (80–250 °C). A summary of the works in which polyalcohol sugars were used as PCMs in direct or indirect solar cookers is given in Table 1.

Table 1. Literature summary of sugar alcohols used experimentally as phase change materials (PCMs) in direct and indirect solar cookers (SCs).

PCM	T_m (°C)	ΔH_m (J/g)	Solar Cooker Design	Cooking Medium	Site	Main Results	Reference
Erythritol	118.0	339.8	Indirect SC with evacuated tube collector (ETC)	Water	Mie, Japan (latitude: 33°48′ N and longitude: 136°2′ E)	Noon cooking did not affect evening cooking. Evening cooking using erythritol was faster than noon cooking.	[13]
Erythritol	118.0	340.0	Concentrating parabolic	Water	Madrid, Spain (latitude: 40°23′ N and longitude: 3°43′ W)	The obtained results indicate that three meals for a family were possible simultaneously with the heat storage both in summer and in wintertime. The storage utensil, left inside an insulating box, allowed to cook dinner and breakfast of the next day with the retained heat.	[14]
Erythritol	118.0	-	Solar electric cooker (SEC)	Water	San Luis Obispo, CA, USA (latitude: 36°46′ N and longitude: 119°25′ W)	The presented prototype was able to boil 1 L of water in less than 20 min with an efficiency of 35%. The SEC coupled with the PCM was able to store heat for more than 4 h.	[15]
Erythritol	117.7	339.8	Solar box cooker	Water and silicone oil	Ancona, Italy (latitude: 43°36′ N and longitude: 13°31′ E)	The TES used in the portable SC stabilized the whole system and extended the use of the prototype when the solar radiation was absent or intermittent. The use of TES resulted in an extension of the average load cooling time by approximately 351% with respect to the system without the TES solution.	[16]
D-Mannitol	167–169	326.8	Indirect SC with parabolic trough collector	Olive oil	Chennai, India (latitude: 12°80′ N and longitude: 80°2′ E)	The experimental data showed that the cooking unit had an efficiency of 73.5% while the overall system efficiency was equal to 10.2%. The main heat losses were identified to be concentrated in the pipes (54.3%), the TES tank (25.3%) and the cooking unit (4.1%).	[17]

It is important to note that SAs can show the phenomenon of supercooling, that is, the latent heat stored in the liquid PCM is released during solidification at a temperature that is lower than the melting point. The supercooling degree of SAs, that is, the difference between the melting and crystallization temperatures, can be more or less severe [18–20] and is influenced by many factors such as the volume size of the sample, the presence of impurities, the container characteristics, and the cooling conditions [21,22]. Supercooling is usually considered a drawback, since it prevents the use of SAs as short-term TESs in different applications [18]. This is especially true for SAs that present high and stable supercooling. For example, it was shown that xylitol remains in a supercooled liquid state even when cooled to temperatures as low as 0 °C, which is very far below its melting point (equal to about 93 °C) [19,20,23,24].

On the other hand, the stable supercooling properties of SAs can be exploited for the development of efficient long-term or seasonal TES systems. In particular, due to its high energy density and high and stable supercooling, xylitol is considered a suitable substance for low to medium temperature applications, ensuring low heat losses due to only sensible heat that reduce insulation costs [25,26]. However, as shown by different experimental and theoretical studies [23,26–29], the use of xylitol as a PCM for TES applications is hindered by its very difficult nucleation triggering and its slow crystal growth rate, resulting in a difficult energy discharge triggering and a low discharge power, respectively.

To overcome these drawbacks, different studies analyzed various techniques to trigger the nucleation and crystallization processes of xylitol and to enhance its crystallization rate. In general, several nucleation triggering methods have been studied to reduce the supercooling degree of various PCMs and to achieve the heat release on demand at the temperature required for the specific application. These techniques are divided into passive—used to reduce supercooling (e.g., the use of additives)–and active, used to trigger the nucleation process (e.g., seeding of crystals of the same substance, use of electrofreezing or ultrasonic waves, local pressure increases, shear techniques, mechanical agitation and bubbling) [30].

To accelerate the crystallization speed of xylitol (i.e., its release rate of latent heat) for its use as long-term HSM, several additives were tested by Seppälä et al. [23] for the reduction of the solid-liquid interface tension and to lower the viscosity of the liquid phase. The obtained results proved that, although some additives gave a substantial increase in the speed of the crystallization front, the crystallization speed of these systems was still lower than that of many other liquids.

Godin et al. [25] experimentally investigated different techniques for the nucleation triggering of highly viscous undercooled xylitol for long-term TES applications. Based on the methods discussed in the paper, the bubbling technique allowed us to efficiently trigger the nucleation of xylitol and to sufficiently accelerate the crystal growth rates. Instead, nucleation triggering techniques (local cooling, seeding, high-power ultrasound) showed very local effects and very low crystallization rates that implied low heat release rates and, consequently, too long discharge times. The authors also stated that, although mechanical agitation is a more intrusive method respect to bubbling requiring an expensive reactor design, it can be considered suitable for the discharge triggering of xylitol at appropriate crystallization rates.

Very similar outcomes were presented in the experimental study by Duquesne et al. [28] concerning the nucleation triggering of undercooled xylitol for long-term TES applications. In particular, the authors proved that two techniques were able to activate and accelerate the crystallization process of severely undercooled xylitol: mechanical agitation and stirring by bubbling using a compressed air reactor. The authors showed that nucleation triggering due to mechanical agitation is very fast, suggesting that this technique could be an efficient solution for discharging the storage system at the appropriate speeds. However, in agreement with Godin et al. [25], it was explained that mechanical agitation exhibited a less homogeneous solidification from a spatial point of view respect to the bubbling method, can be a more intrusive technique, and may require a specific reactor design with

possible extra-costs. On the other hand, the authors explained that stirring by bubbling can be considered a low-intrusive and cost-effective technique that gives a homogeneous solidification from a spatial point of view.

More recently, Delgado et al. [29] experimentally investigated the nucleation triggering of xylitol and the acceleration of its crystallization rate for short-term TES applications. In particular, the authors studied the effect of seeding in presence of shear on the crystallization process of severely undercooled xylitol using both a rheo-optical approach and rheometry. Results showed that the combined effect of seeding and shearing on xylitol can trigger and accelerate its crystallization process.

With the intention of improving the efficiency of solar cookers using natural substances such as SAs, in the present study a portable solar box cooker was tested with a xylitol-based TES. This work continues the authors' research on sugar alcohols combined with solar cookers; in a recent paper, in fact, the same portable solar box cooker was tested with erythritol [16]. Based on the authors' knowledge, there is no study in the literature that involves the use of xylitol as HSM to be used with solar cookers. The purpose of this work is therefore to experimentally characterize a solar box cooker with a xylitol-based TES, in order to evaluate its thermal performance during the heating phase, when solar radiation is available, and during the cooling phase, when solar radiation is not available. To avoid the high and stable supercooling of xylitol and to allow its nucleation triggering at the desired temperature, the TES was equipped with a manual device for the mechanical agitation of the substance. The results obtained using the device for the mechanical agitation of xylitol will be compared with those obtained without considering any nucleation triggering technique. Any possible benefits provided by the studied techniques will be analyzed deeply and discussed.

After the Introduction, the paper is divided into four sections. In Section 2, the experimentally-determined thermodynamic properties of the xylitol sample considered in this work are reported, together with a literature review of its main thermodynamic and transport properties. The TES system used for the tests is also described here, together with the main features of the portable solar box cooker. The same section also reports the experimental parameters that were calculated to characterize the solar cooker system, and the test setup used for the measurements. In Section 3, the results obtained from the experimental tests are provided. Specifically, the following tests are compared: tests carried out without the TES, tests carried out with the TES without using any nucleation triggering technique, and tests carried out with the TES by using the device for the mechanical agitation of the sample. The discussion of the results is provided in Section 4, while Section 5 summarizes the conclusions of the study. Additionally, Appendix A reports a summary of a number of works that studied PCMs with melting point temperatures in the range from 80 to 110 °C for solar cooker applications.

2. Materials and Methods

The system under analysis is composed of two different elements: the portable solar box cooker and the thermal energy storage (TES) containing the heat storage material (HSM) based on xylitol. Firstly, a literature review of the thermal and cycling stability tests performed on xylitol and its main thermodynamic and transport properties is reported, together with different properties measured for the sample used in this work. Then, a detailed description of the TES used in this work is presented, along with the main details of the solar box cooker and of the experimental methodology. Since the optical analysis, the materials and the procedure used for the manufacture of the cooker were extensively described in a previous work [16], in the following subsections only its main properties will be presented.

2.1. Thermodynamic and Transport Properties of Xylitol

Xylitol ($C_5H_{12}O_5$, CAS Number 87-99-0), also called wood sugar, is a sugar alcohol classified as a 5-carbon polyol. It is produced by the metal catalyzed hydrogenation of

the sugar D-xylose [31]. The main substrate for its production is xylan, which is usually extracted from birch, strawberry, raspberry, plum and wheat. It was discovered in 1891 [29,32] and is widely used as a food additive, especially in chewing gums and candies, and in pharmaceuticals. Its sweetening power is similar to that of sucrose, but it contains 40% less calories. In addition, it can prevent the formation of dental caries and arrest initial caries lesions [33]. Two crystalline forms of xylitol are reported in literature: a stable orthorhombic form with a melting temperature in the range 93–94.5 °C and a metastable, hygroscopic monoclinic form with a melting temperature in the range 61–61.5 °C [34,35]. The decomposition temperature of xylitol was determined to be 200 °C [36], that is the highest temperature for its use as a HSM.

Table 2 reports the values of melting temperature (onset, unless otherwise stated), T_m, and latent heat of melting, ΔH_m, which can be found in the literature, measured with a differential scanning calorimeter (DSC). The two properties are necessary for evaluating the potential use of xylitol as an HSM. The collected values of T_m are generally in good agreement, ranging from 92 °C to 95.7 °C, and it is possible to note that they are independent of the heating rate used for the measurement. Instead, slightly higher deviations between the values of ΔH_m can be detected.

The measurements of T_m and ΔH_m for the commercial-grade xylitol charged in the TES of the solar box cooker are reported in Table 2, together with their combined standard uncertainties. The thermodynamic properties were evaluated with the use of a DSC, model NETZSCH DSC 214 Polyma. Adopting a heating rate of 1 °C/min, three different samples of the substance were measured and the average values of T_m and ΔH_m are presented in this study.

The same DSC device, with the same heating rate, was also used to analyze three samples of xylitol with a purity greater than 99% (provided by Sigma-Aldrich). The average values of T_m and ΔH_m are also reported in Table 2. Figure 1 shows the heat flow vs. temperature curves of the average values of the three measurements for the pure xylitol samples and the average values for the commercial-grade xylitol samples. From the results provided in Table 2 and Figure 1, it is possible to state that the values measured for the commercial-grade xylitol used in the TES are consistent with the values measured for the xylitol with a higher purity and those reported in literature.

Table 2. Melting temperature (onset), T_m, and latent heat of melting, ΔH_m, of xylitol measured by DSC at different heating rates (*HR*).

T_m	ΔH_m	*HR*	Purity	Reference
(°C)	(J/g)	(°C/min)	%	
92.0	249.0	0.5	industrial quality	[23]
92.8	241.2	0.5	99	[29]
93.0 ± 1.0	236.0 ± 4.0	0.5	food grade	[37]
92.7	240.1	1	99	[10]
95.1 [a]	251.0	1	99	[11]
92.2 ± 0.1	227.1 ± 1.6	1	commercial grade	this work
92.0 ± 0.5	232.7 ± 9.2	1	99	this work
93.1	226.2	5	≥99	[38]
93.4 ± 0.3	237.5 ± 3.5	5	99	[19]
93.3 ± 0.2	231.4 ± 2.5	5	98	[19]
93.1 ± 1.0	241.0 ± 2.0	5	food grade	[37]
92.7 ± 0.1	232.0 ± 1.0	5	>99	[39]
95.0 [a]	248.0	5	-	[27]
95.0	267.0	10	>98	[40]
93.0	259.7	10	99	[41]
93.0 ± 0.5	263.0 ± 13.0	10	>98	[26]
90.0 ± 1.0	237.6 ± 1.3	10	technical grade	[24]
91.1	286.6	10	-	[42]
94.4 [b]	221.4 ± 2.2	10	>99	[43]
93.0	272.3	10	-	[44]
95.7 [b]	246.0 ± 1.0	-	>99	[45]

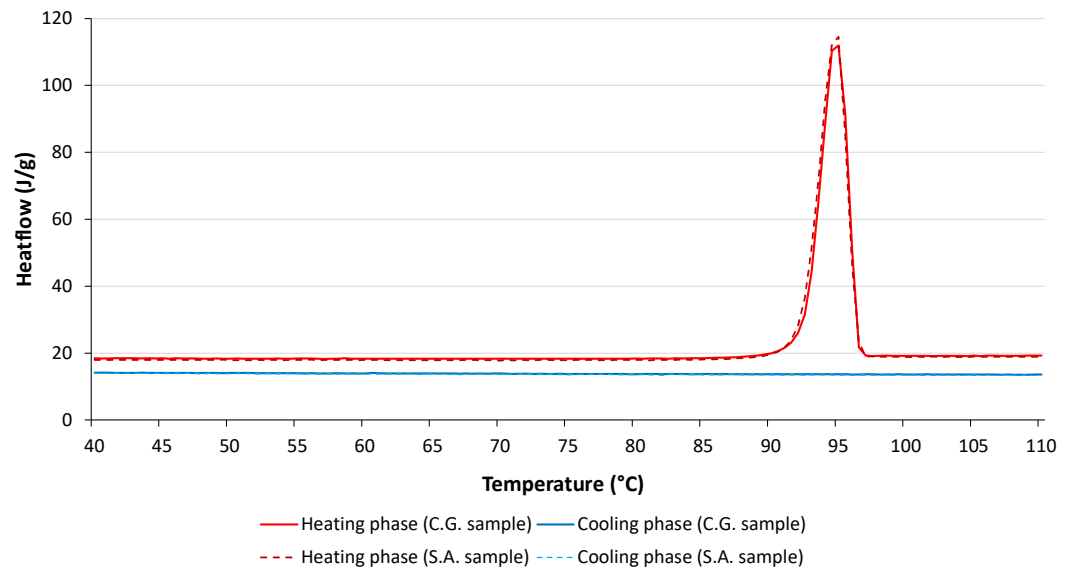[a] unspecified type of temperature. [b] peak temperature.

Figure 1. DSC analysis of commercial-grade xylitol (C.G. sample) and pure xylitol from Sigma Aldrich (S.A. sample).

The absence of an exothermic peak during the cooling phase up to 40 °C is evident in Figure 1 for both the commercial-grade and the pure xylitol samples, demonstrating the lack of crystallization in the DSC tests. In addition, during the heating phase of the following cycle on the same samples, no endothermic peaks were found. This aspect is due to the fact that there was no liquid–solid transition in the cooling phase of the previous cycle. The same results were also obtained by other authors during the cooling phase of the DSC measurements [19,23,24,38,45]. In particular, Shao et al. [19] carried out three consecutive tests and showed that no endothermic peaks were detected in the heating phase of the second and third tests. The lack of crystallization during the cooling phase of melted xylitol was also observed by the same authors with an isothermal test called T-history method [20]. In particular, the authors suggested that xylitol could remain a supercooled liquid until its vitrification at a temperature of −22 °C, at which it could behave like an amorphous glass-like material. The same behavior was also found by Gunasekara et al. [46] with a T-history method and by Höhlein et al. [24] with a three layer calorimeter. Diogo et al. [45] studied the behavior of xylitol resistance to crystallization, linking it to low molecular mobility and a high degree of cooperation in molecular motion. These results prove that xylitol have a very high and stable supercooling, remaining a supercooled liquid at temperatures far below its melting point. Therefore, as mentioned in Section 1, this drawback of xylitol is due to its very difficult nucleation triggering and hinders its direct use for several TES applications. Instead, suitable nucleation triggering methods have to be considered to discharge the energy stored in xylitol at specific temperatures.

Figure 2 shows the regressed and measured values of the specific heat of xylitol available in literature as a function of temperature. From the graph, a general good agreement between the collected values is evident. Figure 3, instead, shows the measured values of the thermal conductivity available in the literature as a function of temperature. In general, from Figure 3, a good agreement is evident in the liquid phase between the different values collected in the literature. The solid phase, however, shows discrepancies.

The values of viscosity (μ) and density measured both in the liquid (ρ_l) and solid (ρ_s) phases for xylitol available in the literature are reported in Table 3, together with their temperature ranges. From Table 3, it can be seen that the percentage change in volume between the solid and liquid states is around 15%, value that should be taken into account when designing a TES system. The same table reveals high values of viscosity, especially at low temperature, which lead to a limited mobility of the molecules and a relevant barrier for nucleation. This phenomenon could partially explain the deep supercooling degree of the substance [26,40]. Finally, it has to be noted that only a very limited amount of

experimental data for viscosity and density of xylitol (with clear values of the temperatures at which the measurements were performed) are available in the literature.

Figure 2. Xylitol specific heat collected from the literature as a function of temperature. The red vertical line indicates the melting temperature and delimits the solid phase (**left**) from the liquid phase (**right**). The points from the work of Zhang et al. [26] at 80 °C and 90 °C refer to the supercooled liquid.
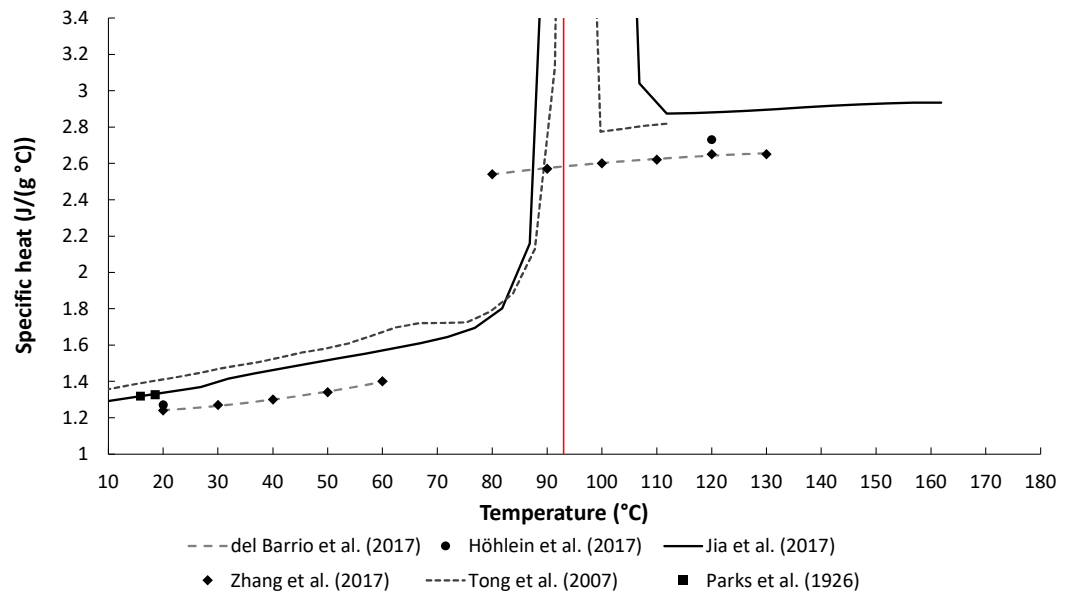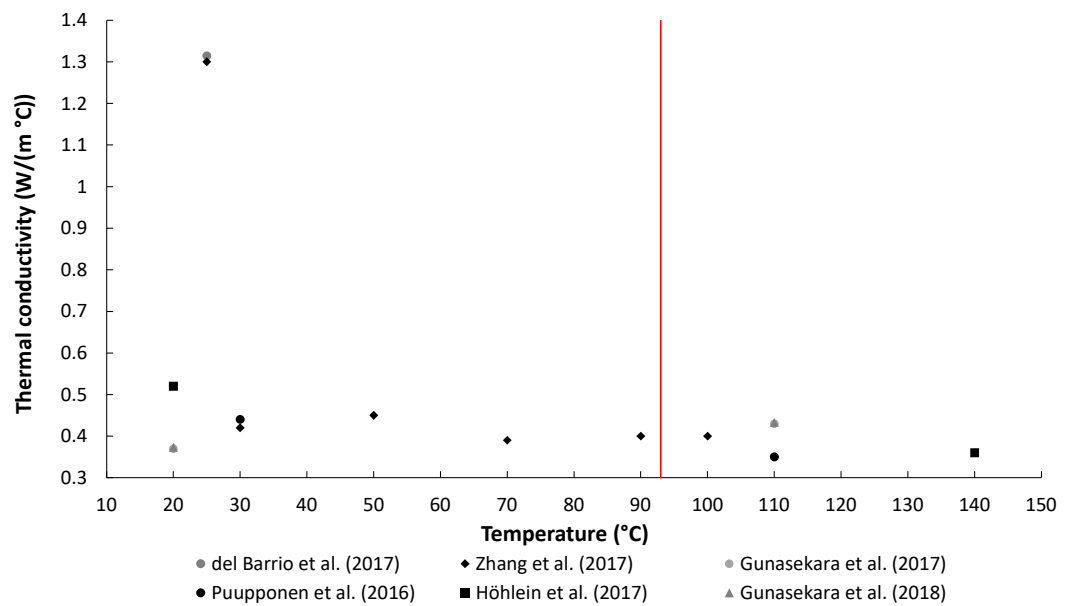

Figure 3. Xylitol thermal conductivity collected from literature as a function of temperature. The red vertical line indicates the melting temperature and delimits the solid phase (**left**) from the liquid phase (**right**). The points from the work of Zhang et al. [26] in the temperature range 30–90 °C refer to the supercooled liquid.

Table 3. Measurements of density in the liquid (ρ_l) and solid (ρ_s) phases and viscosity (μ) of xylitol as a function of temperature collected from the literature.

Quantity	[40]	[26]	[24]	[29]
ρ_s (kg/m^3)	1500.1–1472.5	1497.1–1477.0	1505.0–1487.7	-
T range (°C)	30–90	30–90	20–90	-
ρ_l (kg/m^3)	-	1374.6–1311.5 [a]	1344.6–1324.4	-
T range (°C)	-	40–130	120–150	-
μ (Pa s)	10.01–0.4127	68.05–0.2441	-	0.5
T range (°C)	57–96	40–108	-	90

[a] supercooled liquid.

To the best of the authors' knowledge, the only analysis regarding the thermal performance of xylitol over a long period of application was carried out by Zhang et al. [26] by means of a thermal and cycling stability test. The authors showed that the latent heat of melting of xylitol has decreased by less than 2% after 20 cycles. Unlike other sugar alcohols that showed significant deteriorations of their long-term thermal performance [47–49], these results seem to prove that xylitol has good thermal and cycling performance. However, additional tests characterized by a higher number of cycles are necessary to assess the long-term thermal performance of xylitol in a more accurate way.

2.2. Thermal Energy Storage System

Figure 4 shows the thermal energy storage (TES) chosen to perform the tests. The TES was filled with commercial-grade xylitol and its detailed description can be found in a previous work [16]. In the present work, however, the TES was also equipped with a manual device for the mechanical agitation of the sample, with the aim of triggering xylitol nucleation. The device, highlighted in red in Figure 4, consists of a C-shaped rod able to rotate on the axis of the T-type thermocouple support used to measure the temperature of the testing fluid (T_f). Two thin iron wires (with one end connected to the rod and the other end free, outside the cooking chamber) were used to rotate the rod without opening the cooking chamber. Thanks to its simplicity and ease of use, the device can be considered a cost-effective solution that can be easily implemented in TESs used for solar cookers.
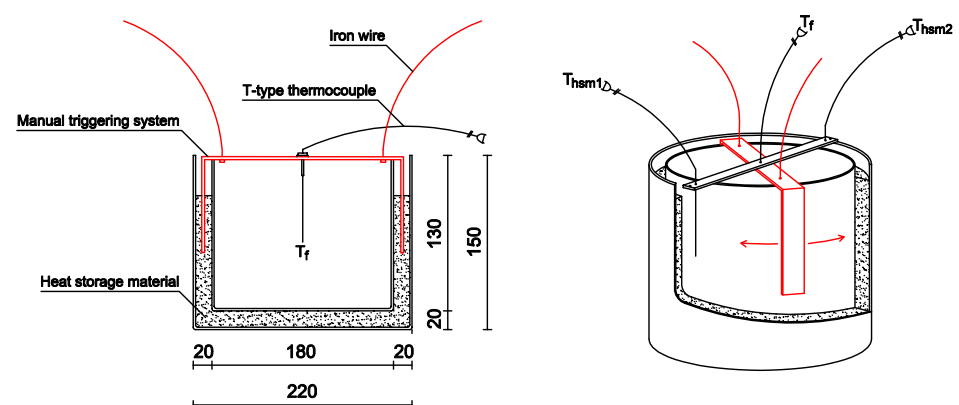
Figure 4. Thermal energy storage. The device used for the mechanical agitation of xylitol is drawn in red.

For the preparation of the heat storage material (HSM), a static oven was used to heat 2.5 kg of commercial-grade xylitol for two hours at over 80 °C. In order to remove any possible moisture from the substance, the same operation was repeated a second time. Whereupon, the HSM was inserted in the TES cavity and the static oven was used to heat the entire system for two hours at a temperature of 150 °C. In addition, before the use of the xylitol-based TES in the solar cooker, several tests were carried out to check the efficiency of the nucleation triggering device. The results proved that the mechanical agitation allowed

the beginning of the crystallization of the sample in a short time and at temperatures close to the melting temperature of xylitol.

2.3. Solar Box Cooker

The portable solar box cooker studied in this work is represented in Figure 5. The concentration ratio of the solar cooker, defined as the ratio between the cooker aperture area and the glass cover area, is equal to 4.08. The prototype has the external part composed of a wooden box, while the internal part includes a zinc-coated steel frame having the function of cooking chamber. The cooking chamber was painted with a selective black coating (SOLKOTE HI/SORB-II), in order to improve its absorptivity to solar radiation (around 90%) and reduce its emissivity in the long wavelength range.

The solar box cooker is thermally insulated with glass wool and the superior part of the cooking chamber is shielded with a tempered glass cover having a transmittance of about 90% and a net surface area of 0.167 m². The cover is surrounded by eight booster mirrors, realized with wooden supports where aluminum foils were glued; the aluminum used for the reflective foils has a solar reflectance of about 94% (MIRO-SUN Weatherproof Reflective 90). The mirrors have two different inclination angles (63.43° and 56.98°, as indicated in Figure 5), and form an aperture area of 0.681 m². A summary of the thermo-optical properties of the solar box cooker and its main characteristics are provided in Table 4.
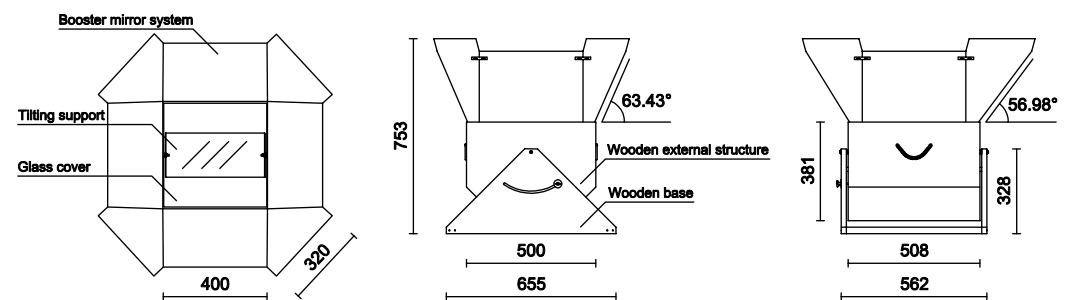

Figure 5. Portable solar box cooker.

Table 4. Thermo-optical properties of the solar box cooker.

Properties	Value
Mass (kg)	20.1
Aperture area, A_a (m²)	0.681
Glass cover area, A_g (m²)	0.167
Concentration ratio, C	4.08
Number of mirrors	8
Inclination angles of mirrors (°)	63.43–56.98
Mirror solar reflectance	0.94
Glass cover solar transmittance	0.90
Black coating solar absorptance	0.90

2.4. Experimental Methodology

The portable solar box cooker under study was tested outdoor on the DIISM (Department of Industrial Engineering and Mathematical Sciences) roof (latitude 43.5867 N, longitude 13.5150 E). To track the sun with good precision, the cooker zenithal and azimuthal alignment were manually adjusted every 5–10 min. Before being tested with the xylitol-based TES, the solar cooker performance was evaluated under no-load conditions and with silicone oil (Rhodorsil Oil 47 V 100), fluid used to exceed the limit of 100 °C given by water boiling.

The main experimental parameters used to characterize the performance of the solar box cooker with and without load are provided in Table 5. For the solar cooker under study, the first figure of merit (F_1), a parameter that indicates the performance of the cooker with no load and in stagnation conditions [50], was found to be equal to 0.19 °C/(W/m²) [16].

Table 5. Experimental parameters for the assessment of the solar cooker performance.

Experimental Parameter	Equation/Formulation	Equation Parameters
First figure of merit [50]	$F_1 = \frac{T_{a,max} - T_{amb}}{DNI}$ (°C/(W/m^2))	A_a = aperture area of the solar cooker (m^2)
		c_f = specific heat of the test fluid (J/(kg K))
Heating time interval	$\Delta t_h = t(T_2) - t(T_1)$ (h)	DNI = direct normal irradiance (W/m^2)
Second figure of merit [50]	$F_2 = \frac{F_1 m_f c_f}{A_a \Delta t_h} \ln \left[\frac{1 - \frac{1}{F_1}(T_1 - T_{amb,av})/DNI_{av}}{1 - \frac{1}{F_1}(T_2 - T_{amb,av})/DNI_{av}} \right]$	DNI_{av} = mean DNI measured at Δt_h (W/m^2)
		$DNI_{ref} = 900\,\text{W/m}^2$
Specific boiling time [51]	$t_s = \frac{\Delta t_h A_a}{m_f}$ (h m^2/kg)	m_f = mass of the test fluid (kg)
		T_{amb} = ambient temperature (°C)
Characteristic boiling time [51]	$t_{ch} = t_s \frac{DNI_{av}}{DNI_{ref}}$ (h m^2/kg)	$T_{a,max}$ = absorber stagnation temperature (°C)
		$T_{amb,av}$ = mean T_{amb} measured at Δt_h (°C)
Overall thermal efficiency [51]	$\eta_{av} = \frac{m_f c_f (T_2 - T_1)}{DNI_{av} A_a \Delta t_h}$	$t(T_1)$ = starting time of the heating phase (h)
		$t(T_2)$ = ending/starting time of the heating/cooling phase (h)
Cooling time interval	$\Delta t_c = t(T_2) - t(T_3)$ (h)	$t(T_3)$ = ending time of the cooling phase (h)

The results of the tests carried out with silicone oil were elaborated again in the present work, in order to define a proper baseline to be used as term of comparison for the tests with the xylitol-based TES. Considering a melting temperature for xylitol equal to 92 °C, each test was subdivided into two phases: a heating phase, evaluated in the range 55–110 °C, where the solar cooker was exposed to solar radiation, and a cooling phase, evaluated in the temperature range 110–80 °C, where the solar cooker was intentionally closed to solar radiation. In this way, it was possible to emulate absence of solar radiation, and to evaluate the thermal behavior of the system with and without the TES.

The main temperatures that characterize the solar box cooker prototype coupled with the xylitol-based TES were measured by means of calibrated thermocouples. T-type thermocouples were installed to measure ambient temperature (T_{amb}) and that of the test fluid (T_f), while K-type thermocouples were used to measure the temperature of the glass (T_g), of the absorber (T_a) and of the HSM ($T_{HSM,1}$ and $T_{HSM,2}$), the latter two inserted in the TES as depicted in Figure 4. Direct normal irradiance (DNI), instead, was measured through a first-class normal incidence pyrheliometer (Epply NIP) mounted on a solar tracker.

3. Results

This section reports the results obtained through the experimental tests carried out with the portable solar box cooker coupled with the xylitol-based TES. The results of the load tests are divided into tests with silicone oil only and tests with silicone oil and xylitol. The latter results are further divided into those obtained without considering any nucleation triggering technique, and those obtained by using the manual device for mechanical agitation.

3.1. Load Tests Carried out with Silicone Oil

Three tests with 1.5 kg of silicone oil were carried out in June 2019. The results derived from the heating phase are provided in Table 6, while the cooling phase is summarized in Table 7 (tests 1–3). The temperatures and the direct normal irradiance detected on 17 June 2019 (test 3) are depicted as an example in Figure 6. Taking as a reference for the heating phase the time required by the silicone oil to take its temperature from 55 to 110 °C (0.71 h), the corresponding average environmental parameters were found to be 28.57 °C for $T_{amb,av}$ and 749.41 W/m^2 for DNI_{av}. The values of the performance parameters discussed in Section 2.4 are provided in Table 6.

Table 6. Summary of the tests carried out with silicone oil and silicone oil + HSM during the heating phase.

Quantity	Test 1	Test 2	Test 3	Test 4	Test 5	Test 6	Test 7	Test 8	Test 9	Test 10
Date	11/06/2019	12/06/2019	17/06/2019	05/06/2019	06/06/2019	07/06/2019	10/05/2021	18/05/2021	20/05/2021	31/05/2021
m_f (kg)	1.5	1.5	1.5	1.5	1.5	1.5	1.5	1.5	1.5	1.5
m_{HSM} (kg)	-	-	-	2.5	2.5	2.5	2.5	2.5	2.5	2.5
T_1 (°C)	55	55	55	55	55	55	55	55	55	55
T_2 (°C)	110	110	110	110	110	110	110	110	110	110
DNI_{av} (W/m^2)	718.69	588.64	749.41	794.45	719.75	726.24	915.76	923.10	946.13	928.17
$T_{amb,av}$ (°C)	30.91	28.17	28.57	28.23	26.97	26.09	24.12	24.08	19.91	21.06
Δt_h (h)	0.83	0.73	0.71	1.68	2.83	2.13	2.28	1.99	2.26	2.36
t_s (h m^2/kg)	0.38	0.33	0.32	0.76	1.28	0.96	1.04	0.91	1.02	1.07
t_{ch} (h m^2/kg)	0.30	0.22	0.27	0.67	1.03	0.78	1.05	0.93	1.08	1.10
η_{av}	0.09	0.13	0.10	0.04	0.03	0.04	0.03	0.03	0.03	0.02
F_2	0.15	0.27	0.17	0.07	0.05	0.06	0.04	0.05	0.04	0.04

Table 7. Summary of the tests carried out with silicone oil and silicone oil + HSM during the cooling phase.

| Quantity	Test 1	Test 2	Test 3	Test 4	Test 5	Test 6	Test 7	Test 8	Test 9	Test 10
Date	11/06/2019	12/06/2019	17/06/2019	05/06/2019	06/06/2019	07/06/2019	10/05/2021	18/05/2021	20/05/2021	31/05/2021
m_f (kg)	1.5	1.5	1.5	1.5	1.5	1.5	1.5	1.5	1.5	1.5
m_{HSM} (kg)	-	-	-	2.5	2.5	2.5	2.5	2.5	2.5	2.5
T_2 (°C)	110	110	110	110	110	110	110	110	110	110
T_3 (°C)	80	80	80	80	80	80	80	80	80	80
$T_{amb,av}$ (°C)	30.36	29.87	28.64	28.08	26.26	26.64	26.41	25.35	19.96	21.44
Δt_c (h)	0.78	0.78	0.69	1.64	2.11	2.00	1.70	3.79	3.23	3.02
Triggering by mixing	-	-	-	-	-	-	-	yes	yes	yes
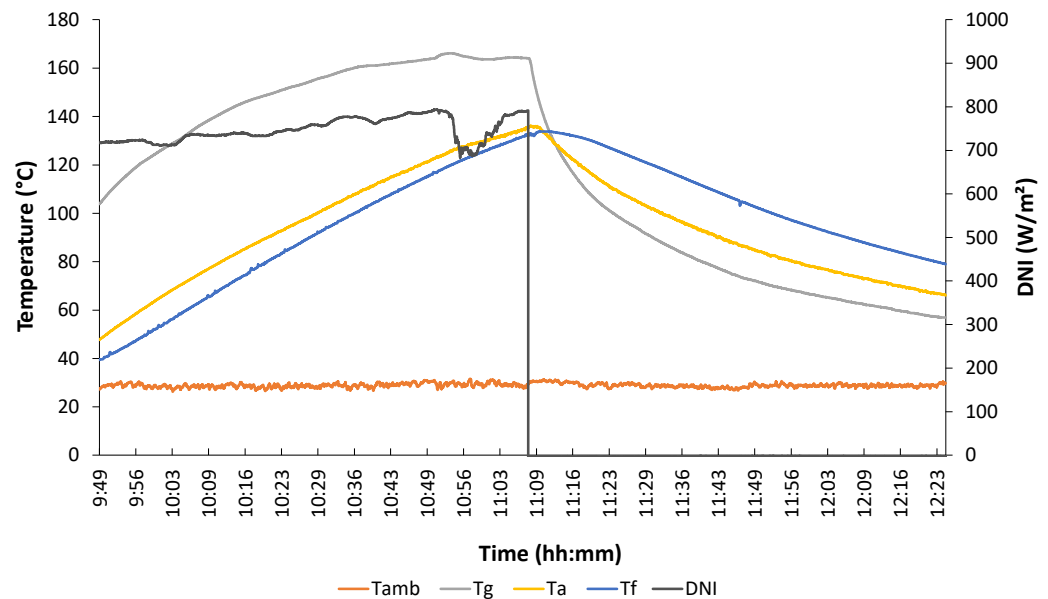
Figure 6. Results of a silicone oil test (17/06/2019, test 3).

Once silicone oil overtook a temperature of 130 °C, the absence of irradiation was emulated by shading the cooker. During the cooling phase, the mean ambient temperature $T_{amb,av}$ was equal to 28.64 °C and silicone oil required around 0.69 h to take its temperature from 110 to 80 °C. As can be verified from Tables 6 and 7, the performance parameters used to characterize the cooker assume repeatable values.

3.2. Load Tests Carried Out with Silicone Oil and Xylitol (without Triggering)

To evaluate the thermal behavior of the solar box cooker integrated with the xylitol-based TES, four outdoor tests with 1.5 kg of silicone oil and 2.5 kg of HSM were performed in June 2019 and May 2021. In the same fashion of the tests carried out with silicone oil only, the results of the experimentation are depicted in Table 6 for the heating phase and in Table 7 for the cooling phase (tests 4–7).

An example of a test carried out with the xylitol-based TES is shown in Figure 7 (test 6). In the heating phase, which required 2.13 h to take the silicone oil temperature from 55 to 110 °C, the mean environmental parameters were $DNI_{av} = 726.24$ W/m^2 and $T_{amb,av} = 26.09$ °C. As evident in Figure 7, the phase transition of xylitol started at about 92 °C, value that corresponds to the melting point of the substance. Due to the presence of the additional mass of xylitol, the heating phase, if compared to test 3 (which has comparable mean environmental parameters), lasted about 200% longer.

The cooling phase, instead, required 2 hours to decrease the test fluid temperature from 110 to 80 °C. During this phase, the mean ambient temperature was 26.64 °C. With respect to the same case evaluated without the xylitol-based TES (test 3, $\Delta t_c = 0.69$ h), the silicone oil cooling time increased by about 190%, allowing a longer thermal stabilization of the test fluid.

Figure 7, however, does not show an evident phase transition for xylitol in the cooling phase, in agreement with the discussion of Figure 1 about the DSC analysis. This phenomenon was observed in all four tests performed with oil + xylitol; the phase change of the HSM occurred only in the heating phase and always around 92 °C. This behavior is probably caused by the fact that xylitol presents crystallization and supercooling issues, as discussed in Section 2.1. Numerous authors have therefore proposed different techniques to promote the nucleation and crystallization behavior of xylitol, such as seeding/shearing, bubbling or mechanical agitation [23,28,29].
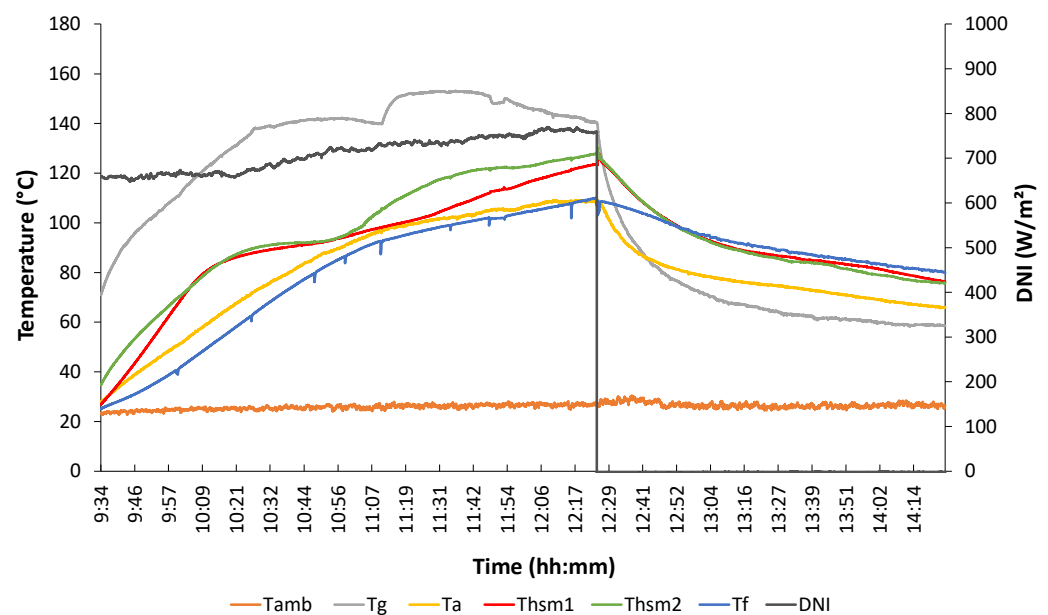
Figure 7. Results of a silicone oil + HSM test without triggering (07/06/2019, test 6).

3.3. Load Tests Carried Out with Silicone Oil and Xylitol (with Triggering)

In addition to the tests carried out without any triggering of crystallization for xylitol, in May 2021 other three investigations were performed with the same methodology (heating + cooling phase), but during the cooling phase the device installed in the TES was manually activated by an operator in order to promote nucleation and, thus, the phase change of the HSM. These tests are also reported in Table 6 for the heating phase and in Table 7 for the cooling phase (tests 8–10).

As can be seen in Figure 8, which shows the test carried out on 20 May 2021 (test 9; $DNI_{av} = 946.13 \, \text{W/m}^2$; $T_{amb,av} = 19.91 \, °C$), no evident difference can be found during the heating stage for the phase change process, that continues to occur at around 92 °C. In the cooling phase, instead, an operator manually triggered for about 5 min the HSM by means of the dedicated device when a temperature lower than the melting point was detected. Looking again at Figure 8, it is possible to note that the manual activation did not result in an immediate response of the substance, which took around 15–20 min to start the phase change process and to increase its temperature. Figure 8 also depicts that the activation process is not uniform in the HSM, but it was faster in a portion of the substance ($T_{HSM,1}$) and slower in another ($T_{HSM,2}$). This effect is likely due to the non-uniformity of the commercial-grade xylitol, but it may also depend on an imperfect utilization of the activation device.

Besides a possible non-uniformity in the activation process, from Figure 8 it is clear that the manual triggering of xylitol allowed to stabilize the thermal capacity of the solar cooker system and, in particular, of the load (silicone oil). This should allow us to extend the cooling time interval and, thus, to improve the thermal performance of the solar cooker when solar radiation is absent or intermittent. This aspect will be discussed in detail in the following section.
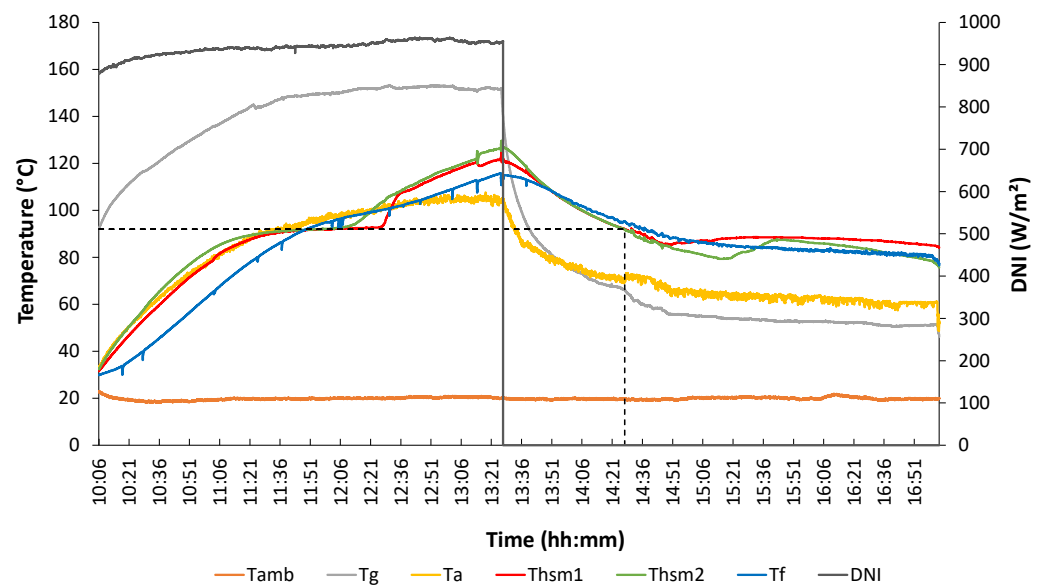
Figure 8. Results of a silicone oil + HSM test with triggering by mixing (20/05/2021, test 9).

4. Discussion

The benefits and disadvantages of using a solar box cooker combined with a xylitol-based TES were quantified by investigating the experimental tests performed with silicone oil (tests from 1 to 3), with silicone oil and HSM without triggering (tests from 4 to 7), and with silicone oil and HSM with triggering (tests from 8 to 10). In all cases, the heating and the cooling sessions were split and elaborated separately. For each test set, it was therefore possible to determine the corresponding heating times ($\Delta t_{h,oil}$ and $\Delta t_{h,oil+HSM}$) and cooling times ($\Delta t_{c,oil}$, $\Delta t_{c,oil+HSM}$ and $\Delta t_{c,oil+HSM,trig}$; in the cooling phase there is a distinction between the tests performed with and without triggering). For the heating phase, the difference between the heating time required for the xylitol-based TES and the time required for the system without TES allows us to determine the time needed to warm-up the material under analysis; this effect is undesired, but unavoidable. For the cooling phase, instead, the same time difference is a desired effect, which should be as high as possible.

Before getting into the discussion, it should be noted that it is not possible to make direct calculations between the heating and the cooling times found for a test. This is true for at least two reasons: (1) during the heating phase, solar radiation provides thermal energy to the HSM, and this causes the phase transition, while during the cooling phase the HSM is left cooling down naturally; (2) the temperature ranges chosen for evaluation are different (55 °C for the heating phase and 30 °C for the cooling phase). It is, however, useful to compare the two times to assess if the useful effect (cooling slowdown of the system) is superior to the detrimental effect (heating slowdown).

Analyzing the heating session, Table 6 shows that the additional mass of HSM implies an increasing heating time, and a general deterioration of the performance parameters. It is also possible to note that Δt_h varies with ambient conditions and may depend on how often the operator acts on the orientation of the solar cooker.

A detailed analysis of the heating time is provided in Table 8. In this table, the mean heating time of the experimental tests performed for silicone oil only ($\Delta t_{h,oil}$, mean value of the Δt_h values reported in Table 6 for the tests 1–3) and for silicone oil and HSM ($\Delta t_{h,oil+HSM}$, mean value of the Δt_h values reported in Table 6 for the tests 4–10) are reported. The corresponding deviation is calculated as the percentage difference between the mean silicone oil + HSM heating time (2.22 h) and the mean silicone oil heating time (0.76 h). As a consequence of that, the solar cooker integrated with the HSM-based TES shows a heating time that is increased by an average 193% with respect to the average performance obtained with the system without HSM. In the same table, the "best" deviation indicates

that, in the most favorable condition, which occurs when the heating time assumes the highest value for silicone oil (test 1, 0.83 h) and the lowest value for silicone oil and xylitol (test 4, 1.68 h), the percentage difference between the two cases is low and equal to 102%. The "worst" deviation, instead, refers to the case which occurs when silicone oil heats up fast (test 3, 0.71 h), while it heats up slowly in the HSM-based TES (test 5, 2.83 h); in this case, the resulting maximum deviation is equal to 299%.

Table 8. Heating time evaluation of the tests with silicone oil and with silicone oil + HSM.

Quantity	Average	Best	Worst
$\Delta t_{h,oil}$ (h)	0.76 (tests 1–3)	0.83 (test 1)	0.71 (test 3)
$\Delta t_{h,oil+HSM}$ (h)	2.22 (tests 4–10)	1.68 (test 4)	2.83 (test 5)
Deviation (%)	193	102	299

The cooling times recorded during the cooling phase of the outdoor tests are reported in Table 7. In this case, the cooling time Δt_c is influenced by the ambient temperature and the manual triggering. As expected, the use of the xylitol-based TES brings to a clear extension of the test fluid thermal stabilization, extension that is even larger when the triggering procedure is performed.

In the same fashion of Table 8, the mean cooling times of the tests carried out with silicone oil only ($\Delta t_{c,oil}$, mean value of the Δt_c provided in Table 7 for the tests 1–3), with silicone oil and HSM without triggering ($\Delta t_{c,oil+HSM}$, mean value of the Δt_c provided in Table 7 for the tests 4–7), and for silicone oil and HSM with triggering ($\Delta t_{c,oil+HSM,trig}$, mean value of the Δt_c reported in Table 6 for the tests 8–10) are provided in Table 9. The table highlights that, when xylitol is not triggered, the mean deviation is equal to 148%, while the "best" condition, which is obtained for test 3 (silicone oil only, 0.69 h) and test 5 (silicone oil and HSM, 2.11 h), results in a maximum deviation equal to 206%. The "worst" case, instead, takes into account the longest cooling time for silicone oil (test 2, 0.78 h) and the shortest cooling time for silicone oil and HSM (test 4, 1.64 h), resulting in a minimum deviation of 110%.

Table 9. Cooling time evaluation of the tests with silicone oil and with silicone oil + HSM (with and without triggering).

Quantity	Average	Best	Worst
$\Delta t_{c,oil}$ (h)	0.75 (tests 1–3)	0.69 (test 3)	0.78 (test 2)
$\Delta t_{c,oil+HSM}$ (h)	1.86 (tests 4–7)	2.11 (test 5)	1.64 (test 4)
$\Delta t_{c,oil+HSM,trig}$ (h)	3.35 (tests 8–10)	3.79 (test 8)	3.02 (test 10)
Deviation w/o triggering (%)	148	206	110
Deviation with triggering (%)	346	449	287
Deviation between trig. and w/o trig. (%)	80	80	84

Even if the use of the xylitol-based TES without triggering has an advantageous effect on the thermal stabilization of the cooking load, a comparison between Tables 8 and 9 depicts that the extension of the heating time is not well counterbalanced by the increase of the cooling time. The absence of manual triggering is therefore not beneficial for a solar cooker using xylitol as HSM, because the two times are comparable. In fact, it is not so useful to extend the cooling time if the heating time is extended by a similar amount.

The issue can be overcome triggering the HSM by mixing. In fact, looking again at Table 9, it is possible to note that deviations when xylitol is manually triggered are much better. In the average case, for instance, the cooling time deviation between the system with its TES triggered and the system without TES is 346%. In other words, the activation of xylitol extends the cooling time period by 80% with respect to the case without activation. Manual triggering allows to achieve an advantageous difference between cooling and heating times, since it allows to take full advantage of the thermodynamic properties of xylitol, that is, its high latent heat of solidification. With the mixing technique, xylitol can

therefore be regarded not just as a generic HSM, but as a PCM in all respects. In this way, even in the worst-case scenario, the use of the xylitol-triggered TES noticeably improves the thermal stabilization of the cooking load.

In particular, considering that the lowest temperature necessary for cooking many kinds of food is around 75 °C [52,53], the extension of the heating time provided by the xylitol-triggered TES can allow us to cook different kinds of food by keeping the temperature in the range 90–80 °C for a long time. Moreover, the system based on xylitol is one of the few TESs that can be exploited in simple and low-cost solar cookers that reach stagnation temperatures of about 100 °C (e.g., the solar cookers proposed by Kesarwani et al. [54], Adewole et al. [55] and Saravanan and Janarathanan [56]).

5. Conclusions

In this paper, xylitol was studied as a heat storage material (HSM) for a portable solar box cooker that has a concentration ratio of 4.08. The results obtained with two configurations (with silicone oil only and with silicone oil and xylitol) were compared and it was found that the average cooling time of the load in the range 110–80 °C was about 148% longer than that evaluated without the xylitol-based thermal energy storage (TES).

Although interesting, this result did not sufficiently counterbalance the increase in the heating time given by the presence of the TES. This was due to a supercooling phenomenon that occurs in xylitol, an issue that prevents the release of thermal energy stored in the liquid phase of the substance. A manual device was therefore installed in the TES to allow the activation of nucleation and crystallization by mixing. The use of the mixing device allowed us to take full advantage of the latent heat of the solidification of xylitol, giving the possibility to regard xylitol as an actual phase change material (PCM). Based on the results of the analysis, the activation technique allowed us to further extend the cooling period by an average 80%, a value that guaranteed an advantageous difference between cooling and heating times.

Given the easy and low-cost nature of the mixing device, its use fits well with solar box cookers meant for developing countries. Even if the device was found to be effective for the system under study, it should be noted that a certain degree of supercooling is still present and nucleation is not totally uniform in the substance. These issues could be solved with a more sophisticated mixing device, or by lying to different activation systems such as bubbling, which showed interesting results in a number of published papers.

Author Contributions: Conceptualization, G.C.; Data curation, A.A., S.T. and P.F.M.; Investigation, G.C., A.A. and S.T.; Methodology, G.C.; Project administration, G.D.N.; Supervision, G.C. and G.D.N.; Validation, G.C., A.A. and S.T.; Writing—original draft, G.C., A.A., S.T. and P.F.M.; Writing—review & editing, G.C., S.T. and P.F.M. All authors have read and agreed to the published version of the manuscript.

Nomenclature

Latin Symbols

A	Area (m^2)
C	Concentration ratio
c	Specific heat (kJ/(kg K))
DNI	Direct normal irradiance (W/m^2)
F_1	First figure of merit (°C/(W/m^2))
F_2	Second figure of merit
HR	Heating rate (°C/min)

m	Mass (kg)	
T	Temperature (°C)	
t	Time (s)	
Greek Symbols		
Δ	Delta difference	
Δ*H*	Latent heat (J/g)	
η	Thermal efficiency	
μ	Viscosity (Pa s)	
ρ	Density (kg/m^3)	
Subscripts		
a	Absorber, aperture	
amb	Ambient	
av	Average	
c	Cooling	
ch	Characteristic	
f	Fluid	
g	Glass	
h	Heating	
l	Liquid	
max	Maximum	
m	Melting	
ref	Reference	
s	Specific, solid	
trig	Triggering	
Acronyms		
DIISM	Department of Industrial Engineering and Mathematical Sciences	
DSC	Differential scanning calorimeter	
HSM	Heat storage material	
PCM	Phase change material	
SA	Sugar alcohol	
SC	Solar cooker	
TES	Thermal energy storage	

Appendix A. Properties of PCMs Used in Solar Cooker Applications at Low Temperature

Table A1 summarizes some of the main works that studied phase change materials (PCMs) with melting point temperatures in the range from 80 to 110 °C for solar cooker applications. From the table, it is possible to note that xylitol has one of the highest latent heat of melting and, unlike other materials, does not have any safety issue.

Table A1. Summary of PCMs used in solar cooker applications at low temperature.

PCM	Material	T_m (°C)	ΔH_m (J/g)	Safety Features	Solar Cooker Design	Reference
Acetamide	Organic	82	263	Probably flammable [a] Toxic [a]	Direct solar stove integrated with fan and reflector	Abu-Hamdeh and Alnefaie [57]
Acetamide	Organic	82	263	Probably flammable [a] Toxic [a]	Direct box-type SC	Sharma et al. [58]
Paraffin wax	Paraffin	83	-	Flammable Non-toxic	Direct box-type SC with 3 inner reflectors	Arabacigil et al. [59]
Paraffin wax	Paraffin	80	220	Flammable Non-toxic	Indirect SC with parabolic dish collector	Senthil [60]
Paraffin wax	Paraffin	100	140	Flammable Non-toxic	Direct concentrating parabolic SC	Lecuona et al. [14]
HS 89	Salt hydrate	88–89	180	-	Direct box-type SC	Bhandari et al. [61]
Magnesium nitrate hexahydrate	Salt hydrate	89	134	Oxidizer [a] Irritant [a]	Indirect SC with external solar collector	Hussein et al. [62]
Magnesium nitrate hexahydrate	Salt hydrate	89	163	Oxidizer [a] Irritant [a]	Direct SC with two concentric cylindrical containers	Domanski et al. [52]
Xylitol	Organic	92	227	Non-flammable Non-toxic	Direct box-type SC	This work

[a] Kim et al. [63].

References

1. Cuce, E.; Cuce, P. A comprehensive review on solar cookers. *Appl. Energy* **2013**, *102*, 1399–1421. [CrossRef]
2. Kundapur, A. *A Treatise on Solar Cookers*, 1st ed.; International Alternate Energy Trust: Udupi, India, 2018.
3. Batchelor, S.; Brown, E.; Scott, N.; Leary, J. Two birds, one stone–Reframing cooking energy policies in Africa and Asia. *Energies* **2019**, *12*, 1591. [CrossRef]
4. Wu, J.; Long, X.F. Research progress of solar thermochemical energy storage. *Int. J. Energy Res.* **2015**, *39*, 869–888. [CrossRef]
5. Abokersh, M.H.; Osman, M.; El-Baz, O.; El-Morsi, M.; Sharaf, O. Review of the phase change material (PCM) usage for solar domestic water heating systems (SDWHS). *Int. J. Energy Res.* **2018**, *42*, 329–357. [CrossRef]
6. Ndukwu, M.C.; Bennamoun, L.; Simo-Tagne, M. Reviewing the Exergy Analysis of Solar Thermal Systems Integrated with Phase Change Materials. *Energies* **2021**, *14*, 724. [CrossRef]
7. Mofijur, M.; Mahlia, T.M.I.; Silitonga, A.S.; Ong, H.C.; Silakhori, M.; Hasan, M.H.; Putra, N.; Rahman, S. Phase change materials (PCM) for solar energy usages and storage: An overview. *Energies* **2019**, *12*, 3167. [CrossRef]
8. Malik, M.S.; Iftikhar, N.; Wadood, A.; Khan, M.O.; Asghar, M.U.; Khan, S.; Khurshaid, T.; Kim, K.C.; Rehman, Z.; Rizvi, S. Design and Fabrication of Solar Thermal Energy Storage System Using Potash Alum as a PCM. *Energies* **2020**, *13*, 6169. [CrossRef]
9. Omara, A.A.; Abuelnuor, A.A.; Mohammed, H.A.; Habibi, D.; Younis, O. Improving solar cooker performance using phase change materials: A comprehensive review. *Sol. Energy* **2020**, *207*, 539–563. [CrossRef]
10. Diarce, G.; Gandarias, I.; Campos-Celador, A.; García-Romero, A.; Griesser, U. Eutectic mixtures of sugar alcohols for thermal energy storage in the 50–90 C temperature range. *Sol. Energy Mater. Sol. Cells* **2015**, *134*, 215–226. [CrossRef]
11. Del Barrio, E.P.; Cadoret, R.; Daranlot, J.; Achchaq, F. New sugar alcohols mixtures for long-term thermal energy storage applications at temperatures between 70 C and 100 C. *Sol. Energy Mater. Sol. Cells* **2016**, *155*, 454–468. [CrossRef]
12. Maldonado, J.M.; Fernández, Á.G.; Cabeza, L.F. Corrosion assessment of myo-inositol sugar alcohol as a phase change material in storage systems connected to Fresnel solar plants. *Molecules* **2019**, *24*, 1383. [CrossRef] [PubMed]
13. Sharma, S.; Iwata, T.; Kitano, H.; Sagara, K. Thermal performance of a solar cooker based on an evacuated tube solar collector with a PCM storage unit. *Sol. Energy* **2005**, *78*, 416–426. [CrossRef]
14. Lecuona, A.; Nogueira, J.I.; Ventas, R.; Legrand, M. Solar cooker of the portable parabolic type incorporating heat storage based on PCM. *Appl. Energy* **2013**, *111*, 1136–1146. [CrossRef]
15. Unger, J.B.; Christler, N.R.; Weeman, M.; Strutz, M.E. *Insulated Solar Electric Cooker with Phase Change Thermal Storage Medium*; Department of Mechanical Engineering, California Polytechnic State University: San Luis Obispo, CA, USA, 2019.
16. Coccia, G.; Aquilanti, A.; Tomassetti, S.; Comodi, G.; Di Nicola, G. Design, realization, and tests of a portable solar box cooker coupled with an erythritol-based PCM thermal energy storage. *Sol. Energy* **2020**, *201*, 530–540. [CrossRef]
17. Kumaresan, G.; Vigneswaran, V.; Esakkimuthu, S.; Velraj, R. Performance assessment of a solar domestic cooking unit integrated with thermal energy storage system. *J. Energy Storage* **2016**, *6*, 70–79. [CrossRef]
18. Nakano, K.; Masuda, Y.; Daiguji, H. Crystallization and melting behavior of erythritol in and around two-dimensional hexagonal mesoporous silica. *J. Phys. Chem. C* **2015**, *119*, 4769–4777. [CrossRef]
19. Shao, X.F.; Wang, C.; Yang, Y.J.; Feng, B.; Zhu, Z.Q.; Wang, W.J.; Zeng, Y.; Fan, L.W. Screening of sugar alcohols and their binary eutectic mixtures as phase change materials for low-to-medium temperature latent heat storage.(1): Non-isothermal melting and crystallization behaviors. *Energy* **2018**, *160*, 1078–1090. [CrossRef]
20. Shao, X.F.; Yang, S.; Wang, C.; Yang, Y.J.; Wang, W.J.; Zeng, Y.; Fan, L.W. Screening of sugar alcohols and their binary eutectic mixtures as phase change materials for low-to-medium temperature thermal energy storage.(2): Isothermal melting and crystallization behaviors. *Energy* **2019**, *180*, 572–583. [CrossRef]
21. Rathgeber, C.; Miró, L.; Cabeza, L.F.; Hiebler, S. Measurement of enthalpy curves of phase change materials via DSC and T-History: When are both methods needed to estimate the behaviour of the bulk material in applications? *Thermochim. Acta* **2014**, *596*, 79–88. [CrossRef]
22. Marín, J.M.; Zalba, B.; Cabeza, L.F.; Mehling, H. Improvement of a thermal energy storage using plates with paraffin—Graphite composite. *Int. J. Heat Mass Transf.* **2005**, *48*, 2561–2570. [CrossRef]
23. Seppälä, A.; Meriläinen, A.; Wikström, L.; Kauranen, P. The effect of additives on the speed of the crystallization front of xylitol with various degrees of supercooling. *Exp. Therm. Fluid Sci.* **2010**, *34*, 523–527. [CrossRef]
24. Höhlein, S.; König-Haagen, A.; Brüggemann, D. Thermophysical characterization of $MgCl_2 \cdot 6H_2O$, xylitol and erythritol as phase change materials (PCM) for latent heat thermal energy storage (LHTES). *Materials* **2017**, *10*, 444. [CrossRef] [PubMed]
25. Godin, A.; Duquesne, M.; del Barrio, E.P.; Achchaq, F.; Monneyron, P. Bubble agitation as a new low-intrusive method to crystallize glass-forming materials. *Energy Procedia* **2017**, *139*, 352–357. [CrossRef]
26. Zhang, H.; Duquesne, M.; Godin, A.; Niedermaier, S.; del Barrio, E.P.; Nedea, S.V.; Rindt, C.C. Experimental and in silico characterization of xylitol as seasonal heat storage material. *Fluid Phase Equilibria* **2017**, *436*, 55–68. [CrossRef]
27. Carpentier, L.; Desprez, S.; Descamps, M. Crystallization and glass properties of pentitols. *J. Therm. Anal. Calorim.* **2003**, *73*, 577–586. [CrossRef]
28. Duquesne, M.; Palomo Del Barrio, E.; Godin, A. Nucleation triggering of highly undercooled Xylitol using an air lift reactor for seasonal thermal energy storage. *Appl. Sci.* **2019**, *9*, 267. [CrossRef]

29.   Delgado, M.; Navarro, M.; Lázaro, A.; Boyer, S.A.; Peuvrel-Disdier, E. Triggering and acceleration of xylitol crystallization by seeding and shearing: Rheo-optical and rheological investigation. *Sol. Energy Mater. Sol. Cells* **2021**, *220*, 110840. [CrossRef]

30.   Beaupere, N.; Soupremanien, U.; Zalewski, L. Nucleation triggering methods in supercooled phase change materials (PCM), a review. *Thermochim. Acta* **2018**, *670*, 184–201. [CrossRef]

31.   Grembecka, M. Sugar alcohols—Their role in the modern world of sweeteners: A review. *Eur. Food Res. Technol.* **2015**, *241*, 1–14. [CrossRef]

32.   Mullin, J.W. *Crystallization*; Elsevier: Oxford, UK, 2001.

33.   Scheinin, A.; Mäkinen, K.K.; Ylitalo, K. Turku sugar studies V: Final report on the effect of sucrose, fructose and xylitol diets on the caries incidence in man. *Acta Odontol. Scand.* **1976**, *34*, 179–216. [CrossRef]

34.   Wolfrom, M.; Kohn, E. Crystalline xylitol. *J. Am. Chem. Soc.* **1942**, *64*, 1739. [CrossRef]

35.   Carson, J.; Waisbrot, S.; Jones, F. A new form of crystalline xylitol. *J. Am. Chem. Soc.* **1943**, *65*, 1777–1778. [CrossRef]

36.   Kaizawa, A.; Maruoka, N.; Kawai, A.; Kamano, H.; Jozuka, T.; Senda, T.; Akiyama, T. Thermophysical and heat transfer properties of phase change material candidate for waste heat transportation system. *Heat Mass Transf.* **2008**, *44*, 763–769. [CrossRef]

37.   Puupponen, S.; Mikkola, V.; Ala-Nissila, T.; Seppälä, A. Novel microstructured polyol—Polystyrene composites for seasonal heat storage. *Appl. Energy* **2016**, *172*, 96–106. [CrossRef]

38.   Brancato, V.; Frazzica, A.; Sapienza, A.; Freni, A. Identification and characterization of promising phase change materials for solar cooling applications. *Sol. Energy Mater. Sol. Cells* **2017**, *160*, 225–232. [CrossRef]

39.   Talja, R.A.; Roos, Y.H. Phase and state transition effects on dielectric, mechanical, and thermal properties of polyols. *Thermochim. Acta* **2001**, *380*, 109–121. [CrossRef]

40.   Del Barrio, E.P.; Godin, A.; Duquesne, M.; Daranlot, J.; Jolly, J.; Alshaer, W.; Kouadio, T.; Sommier, A. Characterization of different sugar alcohols as phase change materials for thermal energy storage applications. *Sol. Energy Mater. Sol. Cells* **2017**, *159*, 560–569. [CrossRef]

41.   Jia, R.; Sun, K.; Li, R.; Zhang, Y.; Wang, W.; Yin, H.; Fang, D.; Shi, Q.; Tan, Z. Heat capacities of some sugar alcohols as phase change materials for thermal energy storage applications. *J. Chem. Thermodyn.* **2017**, *115*, 233–248. [CrossRef]

42.   Saikrishnan, V.; Karthikeyan, A.; Selvaraj, B. Experimental study on thermal performance of xylitol in a latent heat storage combined with sensible heat storage. *AIP Conf. Proc.* **2019**, *2161*, 020038.

43.   Tong, B.; Tan, Z.C.; Shi, Q.; Li, Y.S.; Yue, D.T.; Wang, S.X. Thermodynamic investigation of several natural polyols (I): Heat capacities and thermodynamic properties of xylitol. *Thermochim. Acta* **2007**, *457*, 20–26. [CrossRef]

44.   Saikrishnan, V.; Karthikeyan, A.; Laksmisankar, A.; Beemkumar, N. Thermophysical Characteristic Analysis Of Edible Erythritol And Xylitol For Their Use As Phase Change Materials. *Int. J. Sci. Tech.* **2019**, *8*, 644–649.

45.   Diogo, H.P.; Pinto, S.S.; Ramos, J.J.M. Slow molecular mobility in the crystalline and amorphous solid states of pentitols: A study by thermally stimulated depolarisation currents and by differential scanning calorimetry. *Carbohydr. Res.* **2007**, *342*, 961–969. [CrossRef]

46.   Gunasekara, S.N.; Pan, R.; Chiu, J.N.; Martin, V. Polyols as phase change materials for surplus thermal energy storage. *Appl. Energy* **2016**, *162*, 1439–1452. [CrossRef]

47.   Shukla, A.; Buddhi, D.; Sawhney, R. Thermal cycling test of few selected inorganic and organic phase change materials. *Renew. Energy* **2008**, *33*, 2606–2614. [CrossRef]

48.   Singh, D.; Suresh, S.; Singh, H. Graphene nanoplatelets enhanced myo-inositol for solar thermal energy storage. *Therm. Sci. Eng. Prog.* **2017**, *2*, 1–7. [CrossRef]

49.   Salyan, S.; Suresh, S. Study of thermo-physical properties and cycling stability of D-Mannitol-copper oxide nanocomposites as phase change materials. *J. Energy Storage* **2018**, *15*, 245–255. [CrossRef]

50.   Mullick, S.; Kandpal, T.; Saxena, A. Thermal test procedure for box-type solar cookers. *Sol. Energy* **1987**, *39*, 353–360. [CrossRef]

51.   Khalifa, A.; Taha, M.; Akyurt, M. Solar cookers for outdoors and indoors. *Energy* **1985**, *10*, 819–829. [CrossRef]

52.   Domanski, R.; El-Sebaii, A.; Jaworski, M. Cooking during off-sunshine hours using PCMs as storage media. *Energy* **1995**, *20*, 607–616. [CrossRef]

53.   Khalifa, A.; Taha, M.; Akyurt, M. Design, simulation, and testing of a new concentrating type solar cooker. *Sol. Energy* **1987**, *38*, 79–88. [CrossRef]

54.   Kesarwani, S.; Rai, A.K.; Sachann, V. An experimental study on box-type solar cooker. *Int. J. Adv. Res. Eng. Technol.* **2015**, *6*, 1–6.

55.   Adewole, B.; Popoola, O.; Asere, A. Thermal performance of a reflector based solar box cooker implemented in Ile-Ife, Nigeria. *Int. J. Energy Eng.* **2015**, *5*, 95–101.

56.   Saravanan, K.; Janarathanan, B. Comparative study of single and double exposure Box-type solar cooker. *Int. J. Sci. Eng. Res.* **2014**, *5*, 620–624.

57.   Abu-Hamdeh, N.H.; Alnefaie, K.A. Assessment of thermal performance of PCM in latent heat storage system for different applications. *Sol. Energy* **2019**, *177*, 317–323. [CrossRef]

58.   Sharma, S.; Buddhi, D.; Sawhney, R.; Sharma, A. Design, development and performance evaluation of a latent heat storage unit for evening cooking in a solar cooker. *Energy Convers. Manag.* **2000**, *41*, 1497–1508. [CrossRef]

59.   Arabacigil, B.; Yuksel, N.; Avci, A. The use of paraffin wax in a new solar cooker with inner and outer reflectors. *Thermal Sci.* **2015**, *19*, 1663–1671. [CrossRef]

60. Senthil, R. Enhancement of productivity of parabolic dish solar cooker using integrated phase change material. *Mater. Today Proc.* **2021**, *34*, 386–388. [CrossRef]

61. Bhandari, S.; Gupta, G.; Upreti, P.; Negi, M. Performance Comparison of Different Phase Change Materials for Solar Cooking during off Sun Sunshine Hours. In Proceedings of the Twelve International Conference on Thermal Engineering: Theory and Applications, Gandhinagar, India, 23–26 February 2019,

62. Hussein, H.; El-Ghetany, H.; Nada, S. Experimental investigation of novel indirect solar cooker with indoor PCM thermal storage and cooking unit. *Energy Convers. Manag.* **2008**, *49*, 2237–2246. [CrossRef]

63. Kim, S.; Chen, J.; Cheng, T.; Gindulyte, A.; He, J.; He, S.; Li, Q.; Shoemaker, B.A.; Thiessen, P.A.; Yu, B. PubChem in 2021: New data content and improved web interfaces. *Nucleic Acids Res.* **2021**, *49*, D1388–D1395. [CrossRef] [PubMed]